Effect of slurry clogging phenomena on the face stability of slurry-shield tunnels

In-Mo Lee & Sam Lee
Korea University, Seoul, Korea

Ki-Hoon Choi
Dooosan Industrial & Development Co., Ltd., Seoul, Korea

Lakshmi N. Reddi
Kansas State University, Manhattan, KS, U.S.A.

ABSTRACT: In this paper, the slurry penetration was assessed by soil-filter clogging theory to understand the rheological characteristics. The coefficient of fine particle deposition, represented as an indicator of slurry clogging during tunnel construction, was estimated through several series of modeling experiments. Experimental results showed that the ratio of infiltration velocity to the coefficient of particle deposition was reciprocally proportional to the penetration distance and proportional to the stability of tunnel face. It was also found that the critical d_{10} which needs the special additive was 0.75 mm. In addition, considering the advance rate of tunnelling in stability analyses, the study was further to find the relationship between the tunnel advance rate and the stability of working face due to slurry penetration.

1 INSTRUCTIONS

In the slurry shield method; a world widely-used tunnelling method in saturated and shallow soil cover, the stability of working face depends essentially on the rheological characteristics of slurry penetration into ground, and the attention was drawn to it. The benonite-slurry in tunnelling has been studied by Hutchinson et al. (1975), and Fritz et al. (2002), etc. In this paper, considering the clogging effect, the particle transport and deposition equation, proposed by Gruesbeck & Collins (1982), and Reddi & Bonala (1997), has been used, and the variations of face stability, computed by modeling the experimental results using various degrees of slurry concentration and additives, have been studied.

2 SLURRY SHIELD TUNNELLING

2.1 *Membrane model*

The face stability assessment was studied by Anagnostou & Kovari (1994) based on "membrane-model", i.e. the impervious layer should be formed on the tunnel face, acting like a membrane and inhibiting the infiltration. The support force results from the difference in hydrostatic pressure between the slurry and the ground water. Anagnostou & Kovari's paper suggested that the pressure difference was 20 kPa when an internal friction angle of the ground was greater than 30°.

2.2 *Stability assessment with slurry penetration into the ground*

Face stability in ground will be assessed by considering the limit equilibrium of a wedge loaded by a prismatic body (Anagnostou & Kovari 1994). When the suspension penetrates into the ground beyond the wedge block, it exerts its thrust on a soil zone that is not involved in the sliding mechanism.

Anagnostou & Kovari (1994) proposed that the resulting support force S would decrease gradually during penetration of the slurry according to the following equation:

$$\frac{S}{S_0} = 1 - \frac{e}{2D\tan\omega} \quad \text{if } e < D\tan\omega \tag{1a}$$

$$\frac{S}{S_0} = \frac{D}{2e\tan\omega} \quad \text{if } e > D\tan\omega \tag{1b}$$

where S_0 and ω denote the support force of the membrane-model (i.e., at $e = 0$) and inclination of slip surface, respectively (Fig. 1).

3 CLOGGING THEORY

The clogging theory, proposed by Reddi & Bonala (1997), was analyzed to define the infiltration mechanism of suspension.

Figure 2 shows the schematic of filter clogging when the uniform concentration, C_i, of suspension in layer 1 is transported into the z-direction. The governing equation for the particle transport problem for the filter layer may therefore be written as

$$\frac{\partial C}{\partial t} + V\frac{\partial C}{\partial z} + \lambda C = 0 \tag{2a}$$

$$\partial m / \partial t = \lambda C \tag{2b}$$

where, $C =$ mass of fine particle concentrations per unit pore volume, $m =$ mass of fine particles deposited per unit original pore volume, $\lambda =$ deposition coefficient, $V =$ pore velocity (v/n), $v =$ Darcy's velocity, $n =$ porosity after deposition, z, $t =$ space and time coordinates, respectively.

Using the characteristic function, the solution of Equation 2a can be obtained (Reddi & Bonala 1997); the concentrations of fine particles in the pore fluid, $C(z,t)$, in filter layer, may be expressed as

$$C(z,t) = C_i e^{-\lambda z/V} U(t - \frac{z}{V}) \tag{3}$$

where $U(\cdot)$ is the heaviside step function. Substituting $C(z,t)$ from Equation 3 in Equation 2b, the quantity of fine particles deposited in filter per unit original pore volume may be obtained as

$$m(z,t) = \lambda C_i e^{-\lambda z/V}(t - \frac{z}{V}) \tag{4}$$

Because $m(z,t)$ is the quantity of fine particles deposited in filter per unit original pore volume, the weight of fine particles deposited in the filter may be written as

$$W(z,t) = \int_0^z m(z,t) \cdot A_v dz \tag{5}$$

where $A_v =$ the porosity area ($=A \cdot n$). Substituting $m(z,t)$ from Equation 4 in Equation 5, the weight of fine particles deposited in filter may be obtained as

$$W(z,t) = \int_0^z \lambda C_i e^{-\lambda z/V}(t - \frac{z}{V}) \cdot A_v dz \tag{6}$$

From the modeling experiments, we can determine z, V, A, n, C_i, t and $W(z,t)$. Substituting these values in Equation 6 and integrating, the deposition coefficient λ can be obtained.

4 EXPERIMENTAL INVESTIGATION

4.1 *Experimental set-up*

The tunnel face could be described as a soil-filter interface. The filter layer is to simulate the ground ahead of tunnel faces; the suspension to simulate the slurry in slurry tunnel.

The experimental apparatus being used in this study is composed of four parts shown in Figure 3. First part (a) is a pressure control part. The pressure is provided by an air compressor to keep the uniform pressure Δp of 20 kPa according to the study of Anagnostou & Kovari (1994). Second part (b) is a slurry chamber. Third part (c) is a soil-filter chamber. The soil-filter chamber is composed of six sub-chambers in order to measure the deposition weight per depth after a suspension flow. Fourth part (d) is a water chamber.

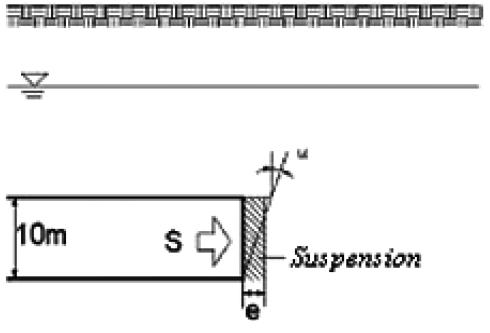

Figure 1. Tunnel section to assess the face stability (Anagnostou & Kovari 1994).

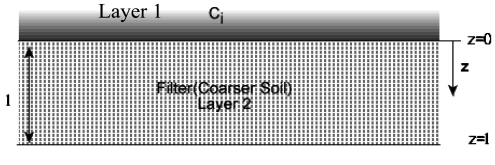

Figure 2. Schematic of filter layers with suspension.

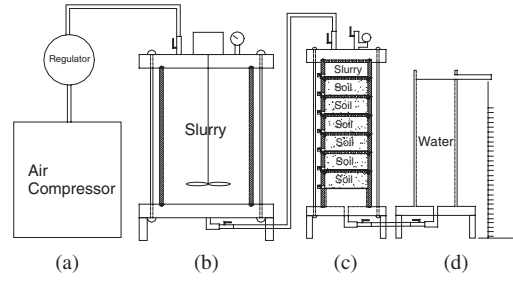

Figure 3. Overall view of the experimental apparatus.

4.2 *Test procedure*

Three types of soil – Soil A, Soil B, and Joomunjin standard sand – were prepared to observe the flow characteristics of slurry as a function of the grain size distribution of the ground. The tests were performed on each type of soils with 6% bentonite-water slurry and several other percentages shown in Table 1.

A series of experiments were performed in the following manner. First, the bentonite-water slurry was prepared at various bentonite concentrations and with additives. Second, the sand was placed in soil-chamber, i.e. approximately 335 grams of soil was filled in each soil sub-chamber using a vibrator. The sand was inundated by slowly percolating water from the bottom to the top; it might be sufficient to simulate in-situ condition. Then, the soil chamber and the water chamber were connected by the tube. After that, the water chamber was filled with the water up to the top level of soil surface. Third, the room above the soil in the soil chamber was filled with the slurry by opening the values. Forth, the constant differential pressure Δp of 20 kPa was applied by the air compressor, controlled by the regulator causing the slurry to penetrate into the soil. The outflow as a function of time and the deposition weight in 6 soil sub-chambers were measured.

4.3 *Soil properties*

The grain size distribution of three soils was shown in Figure 4. Specific gravity *Gs*, porosity *n*, dry unit weight γ_d (kN/m^3), and permeability *k* (cm/sec) of Joomunjin standard sand are 2.65, 0.428, 14.81, and 9.0×10^{-2}, respectively. Those of Soil A are 2.56, 0.417, 14.62, and 3.0×10^{-1}. And those of Soil B are 2.56, 0.417, 14.62, and 1.3×10^{-1}.

5 PARTICLE DEPOSITION COEFFICIENT

5.1 *Fluid loss curve*

The fluid loss curve (the outflow curve of fluid from the soil chamber) is plotted to define the time to begin clogging, and to estimate the particle deposition coefficient with it. The clogging may be developed when the rate of fluid loss was high at the beginning of tests and reduced suddenly as time goes by (see Fig. 5).

A filter cake was formed in Joomunjin standard sand due to a clogging effect at the interface. Soil B also showed appreciable slope reduction when using additives compared to Joomunjin standard sand. However, for Soil A, the fluid loss rate was not reduced at all due to its high permeability.

5.2 *Particle deposition*

The clogging time can be defined as the time when the fluid loss curve meets the asymptotic line as shown in Figure 5, assuming that the deposition weight after

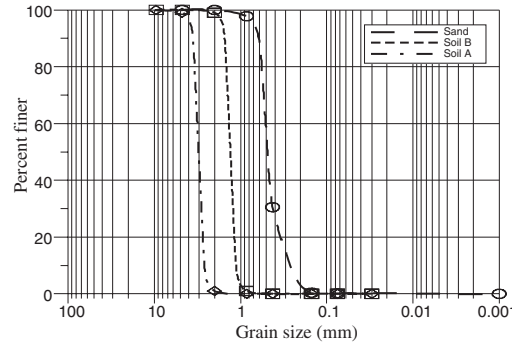

Figure 4. Grain size distribution curve of soils.

Table 1. Experimental results and other calculated variation in Joomunjin standard sand, Soil A, and Soil B.

Soil type	Bentonite conc. (%)	Additive	Pore velocity V(cm/sec)	Deposited weight (g)	Deposition coefficient λ (sec^{-1})	Penetration distance e_{max}(m)	V/λ (cm)	S/S_0 (%)	Safety factor
Joomunjin standard	2%	–	0.29	29.9	8.626×10^{-2}	0.232	3.36	96.8	1.45
	4%	–	0.225	17.26	9.954×10^{-2}	0.156	2.26	97.7	1.47
	6%	–	0.152	20.44	1.577×10^{-1}	0.067	0.96	99.1	1.49
Soil A	6%	–	1.872	53.3	1.382×10^{-2}	9.288	135.5	19.6	0.29
	8%	–	1.85	72.5	1.395×10^{-2}	9.094	132.6	20.0	0.3
	9%	–	1.795	85.11	1.41×10^{-2}	8.73	127.3	20.8	0.31
	8%	1% #100∼#200	1.777	90.72	1.505×10^{-2}	8.10	118.1	22.5	0.34
Soil B	6%	–	0.728	101.74	1.203×10^{-2}	4.145	65	43.9	0.66
	7%	–	0.708	123.68	1.271×10^{-2}	3.817	57.2	47.7	0.72
	6%	1% #100∼#200	0.469	157.95	3.36×10^{-2}	0.961	14.7	86.8	1.30
	6%	1% #40∼#100	0.173	60.62	1.385×10^{-1}	0.086	1.25	98.8	1.48

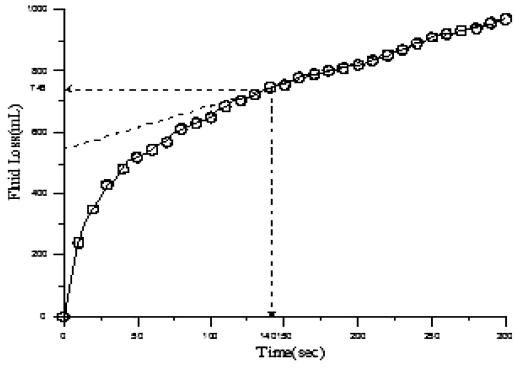

Figure 5. Fluid loss curve for Soil B with 6% bentonite-water slurry plus 1% #40∼#100 additive.

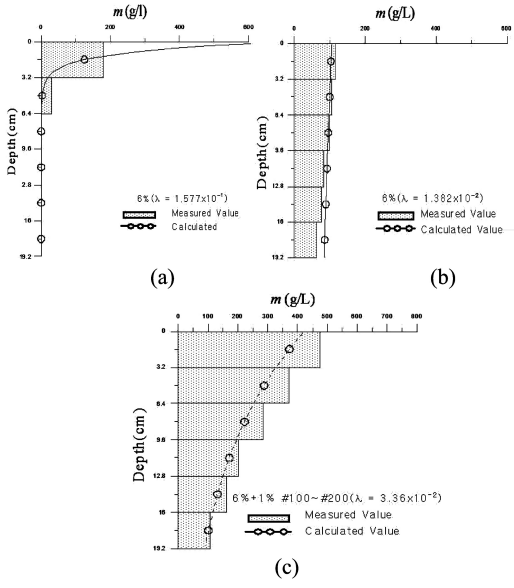

Figure 6. Particle deposition calculated and measured; (a) Joomunjin standard sand and 6% bentonite-water slurry, (b) Soil A and 6% bentonite-water slurry, (c) Soil B and 6% bentonite-water slurry plus 1% #100∼#200 additive.

the completion of test is same as the deposition weight at the clogging time. This is the case when there is no considerable deposition change after the clogging started, which was proved by the experimental results; the estimated values matched well with the measured values shown in Figure 6.

5.3 *Penetration distance*

The penetration distance was defined to be the distance from the tunnel face to the location where the particle

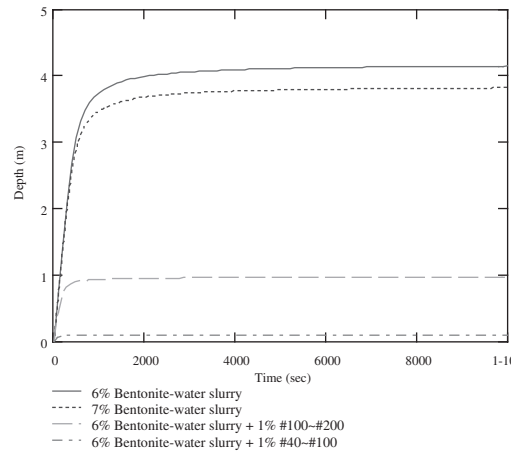

Figure 7. Penetration distance with time (Soil B).

deposition at any time, $m(z,t)$ reaches the following values:

$$m(z,t) = 0.0001 m_0 \tag{8}$$

Figure 7 shows that the penetration distance in Soil B increased suddenly at early time stage and converged quickly as well as Joomunjin standard sand. The converged depth was defined as the maximum penetration distance.

Table 1 shows the experimental results and other calculated variations such as the maximum penetration distance, the deposition coefficient and so on. The maximum penetration distance in Joomunjin standard sand was less than 30 cm; that in Soil A was as large as 9 m. In Soil B, the final penetration distance was about 4 m, but was reduced significantly when mixing the bentonite with additives. It means that the penetration distance is governed by the bentonite concentration and/or mixing additives besides the permeability of the ground. The penetration reduction was achieved more efficiently by employing the additives than by increasing the bentonite concentration.

6 FACE STABILITY ASSESSMENT

6.1 *Support force*

The penetration distances with time being estimated, the support force versus time can be estimated using Equation 1. The safety factor (F_s) and support force are presented in Table 1. The safety factor of membrane model in the example tunnel shown in Figure 1 was 1.5 proposed by Angnostou & Kovari (1994). In case of Joomunjin standard sand, the support force ratios were over about 97%. However, in case of Soil A, these values were significantly reduced down to 20%;

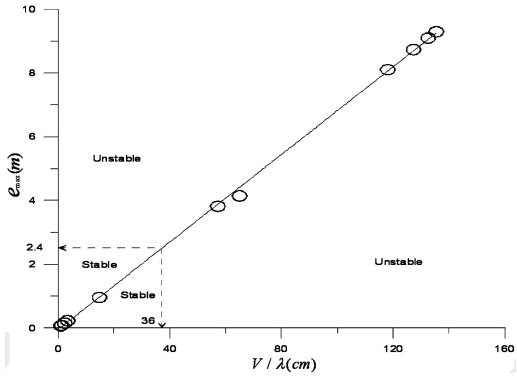

Figure 8. Maximum penetration distance versus V/λ (6% bentonite-water slurry).

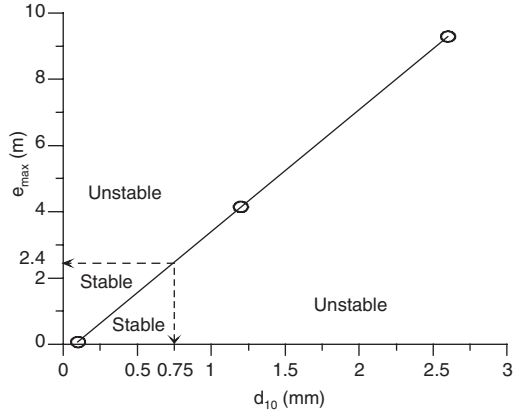

Figure 9. Relationship between maximum penetration distance and d_{10} (6% bentonite-water slurry).

in case of Soil B, these varied largely depending on the slurry concentration and/or by employing the additives.

6.2 *Relationship between V/λ and stability*

Since the deposition coefficient λ is controlled by the pore velocity as well as the soil type, it was normalized with the pore velocity (shown in Table 1) to be used for assessing the tunnel face stability.

As shown in Figure 8, the maximum penetration distance was proportional to V/λ. The critical penetration distance estimated from Equation 1 (i.e. $F_s = 1.0$) was 2.4 m when the safety factor in the membrane model is 1.5. The critical V/λ was about 36 cm when 6% bentonite-water slurry was used.

6.3 *Relationship between d_{10} and stability*

Since an infiltration velocity is related to the particle size distribution, the face stability is highly associated

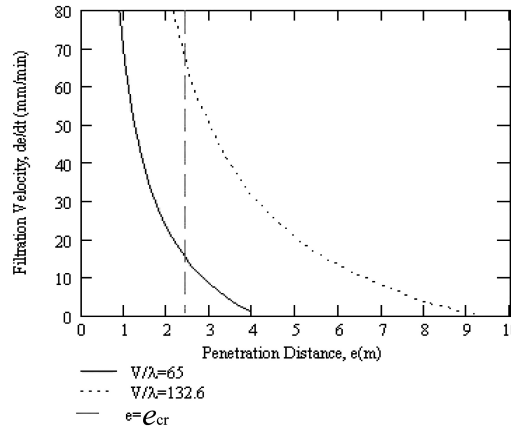

Figure 10. Filtration velocity as a function of penetration distance.

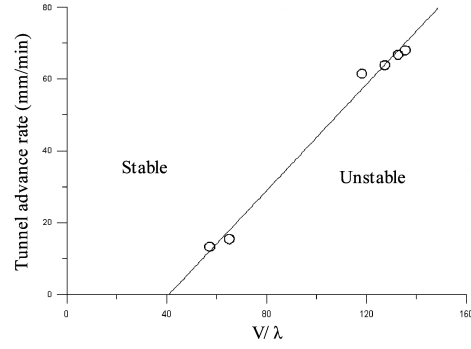

Figure 11. Tunnel advance rate versus V/λ.

with effective size d_{10}, i.e. the grain diameter at which 10% of the soil weight is finer. Adopting this viewpoint, the relationship between maximum penetration distance and d_{10} was drawn in Figure 9.

There was a linear relationship between the maximum penetration distance and d_{10}. The critical penetration distance being 2.4 m, it was drawn that the critical d_{10} was about 0.75 mm. If the effective size d_{10} is over 0.75 mm, mixing with additives or increase in bentonite concentration may be necessary to keep the tunnel face stable.

6.4 *Stability assessment under advance rate*

During the continuous tunnel excavation, a quasi-steady state occurs in which the infiltration velocity is equal to the excavation advance rate (Anagnotou & Kovari 1994). The critical excavation advance rate is defined as

$$u_{cr} = \left(de/dt\right)_{e=e_{cr}} \tag{9}$$

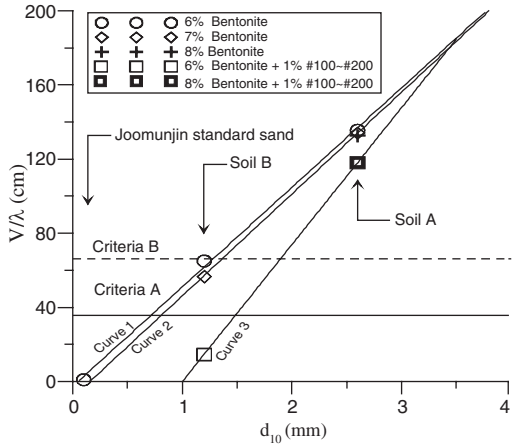

Figure 12. Relationship between V/λ, d_{10} and excavation advance rate (Curve 1: 6% bentonite-water slurry, Curve 2: 7% bentonite-water slurry, Curve 3: 6% bentonite-water slurry plus 1% #100~#200 additive, Criteria A: Criteria without the consideration of advance rate, Criteria B: Criteria with the consideration of advance rate ($u = 20$ mm/min)).

Equation 9 is solved and plotted in Figure 10. The critical advance rate can be obtained from Figure 10 having 2.4 m of critical penetration distance. In this paper, only simplified cases without ground water flow are considered. And the relationship between V/λ and the advance rate was shown in Figure 11.

6.5 *Face stability in slurry shield tunnel*

Figure 12 represents all experimental results explained previously. Curve 1, 2, and 3 are the results tested with 6% bentonite-water slurry, 7% bentonite-water slurry, and 6% bentonite-water slurry added with 1% #100~#200, respectively.

As shown in Figure 12, the point of intersection with horizontal axis was 0.1 mm and 0.2 mm in Curve 1 and 2, respectively. The point of intersection with horizontal axis means the maximum effective size d_{10} in which the membrane can be built up on tunnel face. Thus, the slurry rarely penetrates into the soil using 7% bentonite-water slurry if the effective size d_{10} is lower than 0.2 mm. The higher the concentration and the additive quantity are, the larger the maximum effective size d_{10} to form a membrane is.

Criterion A in Figure 12 is the criterion when V/λ is 36 cm without considering the advanced rate; Criterion B is the one when the advanced rate is 20 mm/min. When the advanced rate is 20 mm/min, the critical effective size d_{10} is about 1.25 mm in 6% bentonite-water slurry which was twice larger than the value when the advanced rate was not considered.

The effective sizes d_{10} in Curve 1, 2, and 3 are 0.7 mm, 0.8 mm, and 1.5 mm, respectively, when the advanced rate is not considered. The one in case of Curve 3 is the largest. Especially, the difference of d_{10} between Curve 1 and 2 is smaller than the one between Curve 1 and 3. It means that the additive is more effective than the concentration increment in the face stability problems.

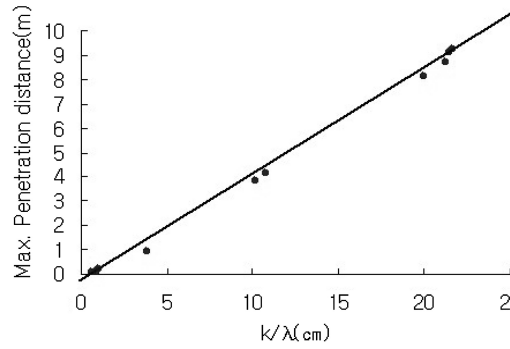

Figure 13. Penetration distance vs. k/λ.

In this paper, the normalized coefficient of deposition V/λ was used to assess the tunnel face stability. For practical purpose, the ratio of the coefficient of permeability to the deposition coefficient (k/λ) can be used since it is easier to obtain in the laboratory testing. Figure 13 shows that there is a linear relationship between e_{max} and k/λ.

7 CONCLUSIONS

The major findings from this study are summarized below:

(1) With increasing the bentonite concentration and employing additives, the deposition coefficient λ is increased, and consequently the infiltration distance of the suspension into the ground is decreased. However, the additive was more efficient than the concentration increment to retain the face stable.
(2) The 6% bentonite slurry had no effect on the support if the effective size d_{10} was over 0.75 mm without additives. Additionally, if the effective size d_{10} was over 1.5 mm, the physical additive (1% #100~#200) had also no effect on the support. In this case, the chemical additive, reacting by a chemical bonding, might be required.
(3) The face stability is not only a function of the deposition coefficient, but also the velocity in the pore and/or the coefficient of permeability.

Chemical additives were beyond the scope of this study. In order for further study to determine the rheological characteristics of slurry with chemical

additives, more parametric study with chemical reaction should be performed with understanding of the complex interrelation.

REFERENCES

Anagnostou, G. & Kovari, K. 1994. The face stability of slurry-shield-driven tunnels, *Tunnelling and Underground Space Technology* 9(No. 2): 165–174.

Fritz, P., Hermanns S.R. & Heinz, A. 2002. Modified bentonite slurries for slurry shields in high permeable soils, *4th International Symposium Geotechnical Aspects of Underground Construction in Soft Ground*: 35–40.

Gruesbeck, C. & Collins, R.E. 1982. Entrainment and deposition of fine particles in porous media. *Society of Petroleum Engineers Journal, December 1982*. 847–856.

Hutchinson, M.T., Daw, G.P., Shotton, P.G. & James, A.N. 1975. The properties of bentonite slurries use in diaphragm walling and their control, *Proceeding of Diaphragm Walls and Anchorages, ICE*: 33–39. London.

Reddi, L.N. & Bonala, M.V.S. 1997. Analytical solution for fine particle accumulation in soil filters. *Journal of Geotechnical and Geoenvironmental Engineering, ASCE* 123(No.12): 1143–1152.